Int. J. Nanosci. Nanotechnol., Vol. 11, No. 3, Sept. 2015, pp. 147-157

Study of Super Capacitive Behavior of Polyaniline/manganese Oxide-Carbon Black Nanocomposites Based Electrodes

M.G. Hosseini [1*], E. Shahryari [1], R. Najjar [1] and I. Ahadzadeh [2]

1. Electrochemistry Research Laboratory, Department of Physical Chemistry, Chemistry Faculty, University of Tabriz, Tabriz, I. R. Iran.

2. Department of organic Chemistry, University of Tabriz, Tabriz, I. R. Iran.

(*) Corresponding author: Mg-hosseini@tabrizu.ac.ir
(Received: 26 June 2014 and Accepted: 02 Sep. 2015)

Abstract
The supercapacitive behavior of polyaniline/MnO_2-carbon black (PANI/MnO_2-CB), MnO_2-CB nanocompositesand CB was studied. MnO_2-CB made by the in situ direct coating method to deposit MnO_2 onto CB; then PANI coating was coated on it. Morphology of the nanocomposite was studied by X-ray diffraction (XRD), Fourier transform infrared (FT-IR) spectroscopy and scanning electron microscopy (SEM). The electrochemical properties of electrodes were investigated by cyclic voltammetry (CV), galvanostatic charge–discharge and electrochemical impedance spectroscopy (EIS) techniques in 0.5 M Na_2SO_4. The specific capacitance of 179.8 F. g^{-1} was obtained for PANI/MnO_2-CB compared with 121 F. g^{-1} for MnO_2-CB and 44.87 F. g^{-1} for CB. The EIS results also revealed improved capacitive properties of CB by the addition of MnO_2 and PANI.
Keywords*: Chemical polymerization, Cycle stability, Life time, PANI/MnO_2-CB, Supercapacitor*

1. INRODUCTION

Electrochemical capacitors, called supercapacitors (SCs), are charge-storage devices that are able to fast charges and discharges (Simon & Gogotsi, 2008, p. 845). The capacitance of these capacitors originate from charging or discharging of electrical double layer (electrical double layer capacitance) or from faradic redox reactions (pseudo capacitance) (Conway, 1991, p. 1539), (Chen*etal*., 2015, p. 495). Double layer capacitors store energy by the separation of opposite charges at the electrode/electrolyte interface whilepseudo capacitors utilizes faradic redox process (Liu*etal*., 2009, p. 678), (Ghennaatian *etal*., 2009, p. 1717). The electrode materials have a very important role in the achievement of high performance super capacitors (Mei *etal*., 2014, p. 36). Different materials have been used in supercapacitors, including (I) carbonous materials(Jian & Tripathi, 2015, p. 1391), (II) conducting polymers, and (III) transition-metal oxides (TMs), conducting polymers (CPs) (Zhang *etal*., 2007, p. 1017) and hybrid systems, carbon/metal oxides/conducting polymers(Konyushenko *etal*., 2008, p. 231). These devices are now better referred as "electrochemical capacitors" rather than double-layer capacitors (Rudge*etal*., 1994, p. 273). MnO_2 is thought of being the most promising transition metal oxide for the successive generation of supercapacitors

because of its high-energy density, low cost, environmental friendliness, and natural abundance (Nam *etal*., 2009, p. 323), (Kim *etal*., 2009, p. 837), whereas one of the important challenges with manganese oxide is its low electrical conductivity. The specific capacitance of thin MnO_2 films is about ~700 F. g^{-1}. However, the specific capacitance gradually decreases with increasing film thickness, and the reported values for the specific capacitance are usually in the range of 100 to 250 F. g^{-1}(Sen & De, 2010, p. 4677). Thus, many approaches have been taken to overcome this disadvantage through synthesizing specific nanostructures (Fischer*etal*., 2008, p. A246), (Wei& Zhitomirsky, 2008, p. 40), (Cheong& Zhitomirsky, 2009, p. 346), or composites with conducting materials. Toward this end, researchers have made great efforts in developing, conducting polymers (CPs) as good candidates for supercapacitor electrode materials due to their unique properties such as facile thin film fabrication, ease of processability, light weight and elasticity (Cho& Lee, 2005, p. 1). Among CPs, polyaniline (PANI) has attracted significant attention, because of its high electroactivity, controllable electrical conductivity and excellent environmental stability (Hu *etal*., 2009, p. 990). Considerable efforts have been made to couple the unique advantages of these capacitive materials for electrochemical capacitor (Kim *etal*., 2006, p. 1697), (Barpanda*etal*., 2009, p. A873), (Fan *etal*., 2007, p. 3083), (Yuan *etal*., 2008, p. 7039).

In the present paper, we report hybrid electrodes in the form of conducting polymer/transition metal oxide/carbon black (CB) nanocomposite prepared in two steps. In the first step manganese oxide was coated on the CB and in the second step PANI was deposited on manganese oxide-coated CB (MnO_2-CB) by oxidation polymerization. The synergistic effect of pseudo capacitive reaction and super capacitive behavior of PANI/MnO_2-CB nanocomposite are discussed. The aim of this work is to study the influence of PANI and MnO_2 particles on the super capacitive behavior of CB. MnO_2 was deposited onto CB by direct coating method and reduction of $KMnO_4$, then, PANI was deposited on it by oxidation polymerization.

The electrochemical performance of PANI/MnO_2-CB, MnO_2-CB and CB electrodes was investigated by electrochemical impedance, cyclic voltammetry and galvanostatic charge–discharge techniques.

2. EXPERIMENTAL

2.1. Materials

CB was used after acid treatment using a sulfuric acid and nitric acid (3:1, v/v) mixture. Ammonium per sulfate (APS) was obtained from Merck. Aniline monomer was distilled prior to use. All other chemicals were of analytical grade and used as received. All electrochemical experiments were carried out at room temperature.

2.2. Procedures

2.2.1. Preparation of MnO_2-CB

According to (Kim *etal*., 2012, p. 2751), first, 1 g of CB was acid-treated under sonication for 2 h and then reacted for 6 h at 80 °C under stirring. Acid-treated CB (A-CB) was washed with water until a pH level of 7.0 was attained. This sample was then filtered and dried at 100 °C. After, 0.5 g of A-CB was mixed with 100 ml of 0.2M $KMnO_4$ solution in a flask. After the reaction, the mixture was filtered and washed with distilled water. The filter cake was dispersed in 200 ml of deionized water followed by the addition of 10 ml of 1M citric acid and then maintained at 160 °C for 12 h under vigorous agitation during the whole course. A condenser was fitted to the reactor to prevent liquid loss by evaporation. Finally, the composite products were filtered, purified with water, and dried.

2.2.2. Preparation of PANI/MnO_2-CB

According to (Kim *etal*., 2012, p. 2751), first, 0.1 g of MnO_2-CB was dispersed in

100 ml of 1M HCl solution under sonication for1 h. Then, 5 ml of the aniline monomer was added to the MnO_2-CB solution with constant stirring. After that, 100 ml of 0.1M APS solution was added drop wise to the above solution for 30 min to initiate oxidation polymerization. The reaction was continued for 24 h at 0 to5°C. The final product was washed and then dried.

2.2.3. Preparation of electrodes

For preparing the working electrodes, sample, carbon black, and poly tetrafluro ethylene (PTFE) were mixed (70:20:10, w/w) and dispersed in N- Methyl pyrolidone (NMP). The mixture was coated on graphite electrode (A=1.0048cm^2), and dried at 100 °C for 12 h.

2.3. Characterization and electrochemical tests

Morphology of the nanocomposite was characterized by a scanning electron microscope (MIRA3FEG-SEM, Tescan). XRD analysis of samples were carried out by a diffractometer (Siemens D5000) with CuK(α) radiation (λ=1.5418A˚). Measurements were conducted in the 2Θrange from 20˚to 80˚. FT-IR spectra were recorded on Perkin-Elmer FT-IR spectrophotometer (4000–450 cm^{-1}). KBr pellet technique was used to prepare sample for recording FT-IR spectrum**.**

The electrochemical experiments were performed in a three electrode cell arrangement. A platinum sheet with a geometric area of about 20 cm^2 was used as counter electrode, and the potentials were measured with respect to an Ag/AgCl reference electrode. Electrochemical experiments were carried out using a Princeton Applied Research, EG&G PARSTAT 2263 Advanced Electrochemical system run by Power Suite software. Cyclic voltammetry measurements were carried out in 0.5 M Na_2SO_4 solution at a scan rate of 10 to 50 $mV.s^{-1}$ and in a voltage range of −1.0 to 1.0 V. Galvanostatic charge/discharge curves were measured at a current density of 0.2 A. g^{-1}.Electrochemical impedance measurements were carried out by applying an AC voltage of 10 mV amplitude in the100 kHz to 10 mHz frequency range. Fit and analysis of EIS data were performed with ZSimTM 3.22 software.

3. RESULTS AND DISCUSSION

3.1. Material characterization

3.1.1. Studies of XRD

The structural features of CB, MnO_2-CB and PANI/MnO_2-CB nanocomposites are determined using XRD (Figure. 1).

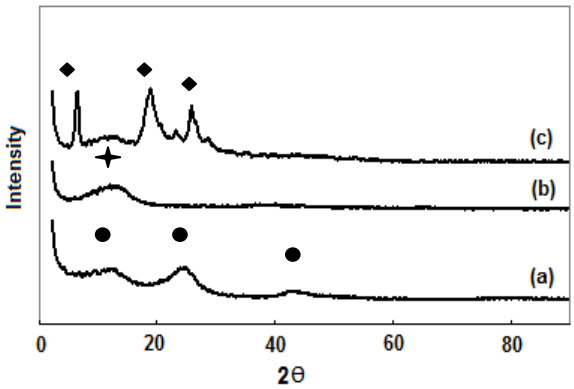

Figure1. *XRD patterns of a) CB, b) MnO_2-CB and c) PANI/MnO_2-CB*

The CB showed a reflection corresponding to (002) peak planes at 2Θ=25° to (Wu *etal*., 2008, p. 483). The two peaks around 2θ=12° and 43° are related to (001) reflections. From Figure 1(b), broad peaks at 2θ =13° can be indexed to brines site-type MnO_2. The diffractions of 2θ = ~15°, 2θ = ~19.4° and 25° can be found in obtained PANI salt. These peaks are related to the emeraldine salt forms of PANI. The crystallinity of PANI can be ascribed to the repetition of benzenoid and quinoid rings in PANI chains. The peak at θ = ~19.4° may be ascribed to a periodicity parallel to the polymer chain, and the peak at 2θ = ~25°may be caused by the periodicity perpendicular to the polymer chain (Shao *etal*., 2012, p. 483). The peak at 2θ = ~20° indicates the characteristic distance between the ring planes of benzene rings near chains.

3.1.2. Studies of FTIR

Figure 2 shows the FT-IR spectra of acid functionalized CB, MnO_2-CB and PANI/MnO_2-CBnanocomposites. The acid functionalized CB spectrum (Figure 2(a)) shows one peak at around 1700cm^{-1} which is related to the presence of C=O stretching mode of carboxylic groups.

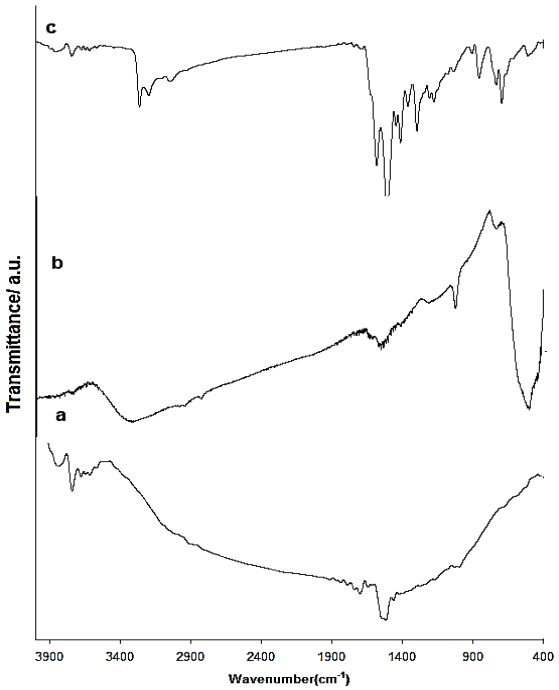

Figure2. *FTIR spectrum of a) CB, b) MnO_2-CB and c) PANI/MnO_2-CB*

The peak signal appeared at 3800 cm^{-1} is associated with the OH group of carboxylic acid. From Figure 2 (b) the broadband at around 3400cm^{-1} and the one between 400 and 800cm^{-1} are attributed to the stretching vibrations of H–O–H and Mn–O bending vibration, respectively. Several small absorption peaks at around 1000–1500cm^{-1} are attributed to the bending vibrations of O–H bonds. The FT-IR spectrum of PANI/MnO_2-CBnanocomposite (Figure 2(c)) has peaks at 1581cm^{-1}(assigned as C=C stretching of the quinoid rings), 1413 cm^{-1}(C=C stretching deformation of benenzoid ring), 1294 cm^{-1} (C–N stretching of secondary aromatic amine), 1145 cm^{-1} (N–N quinoid) and 825 cm^{-1} (out-of-plane deformation C–H in the benzene ring) (Mirmohseni *etal*., 2012, p. 182). The interactions between the conjugated structure of CB and the quinoid rings of PANI molecules increases the degree of charge delocalization on the polymer backbone. It can be seen that in the PANI/MnO_2-CB spectrum, the Mn-O peak intensity reduces. It may be due to the PANI coating on the MnO_2-CB nanocomposite.

3.2. Morphology characterization

Figure 3 shows the SEM images of the nanocomposite. From Figure 3(a), CB is made up of somewhat spherical aggregates about (200-400 nm), each aggregate being made up of particles of about 24 nm. From Figure 3(b)it can be seen that the particles which are in the range of 30 and 60 nm are agglomerated to form larger aggregations. MnO_2 nanoparticles appeared as bright deposits on the CB particles. Figure 3(c) exhibits the SEM image of the PANI/MnO_2-CB composite. It is clear that this composite is composed of some blades which have formed in sphere like structures.
Figure 4 shows the EDS analysis of the MnO_2-CB nanocomposite and CB. The elemental components of the nanocomposite are also inserted in table 1.

3.2.1. Cyclic Voltammetry studies

Figure 5 shows the cyclic voltammetry of electrodes. It is obvious that the current density of CB increased by the incorporation of MnO_2 nanoparticles. Furthermore, the current density of MnO_2-CB also increased by application of PANI. The voltammograms of CB and MnO_2-CB is featureless, almost rectangular and has symmetric characteristics of a supercapacitor (Wang *etal*., 2011, p. 5413).

The proposed mechanism for the charge storage in MnO_2 electrode is adsorption/desorption of Na^+ from the electrolyte.

$$(MnO_2)_{surface} + Na^+ + e^- \rightleftarrows (MnO_2^-Na^+)_{surface} \qquad (1)$$

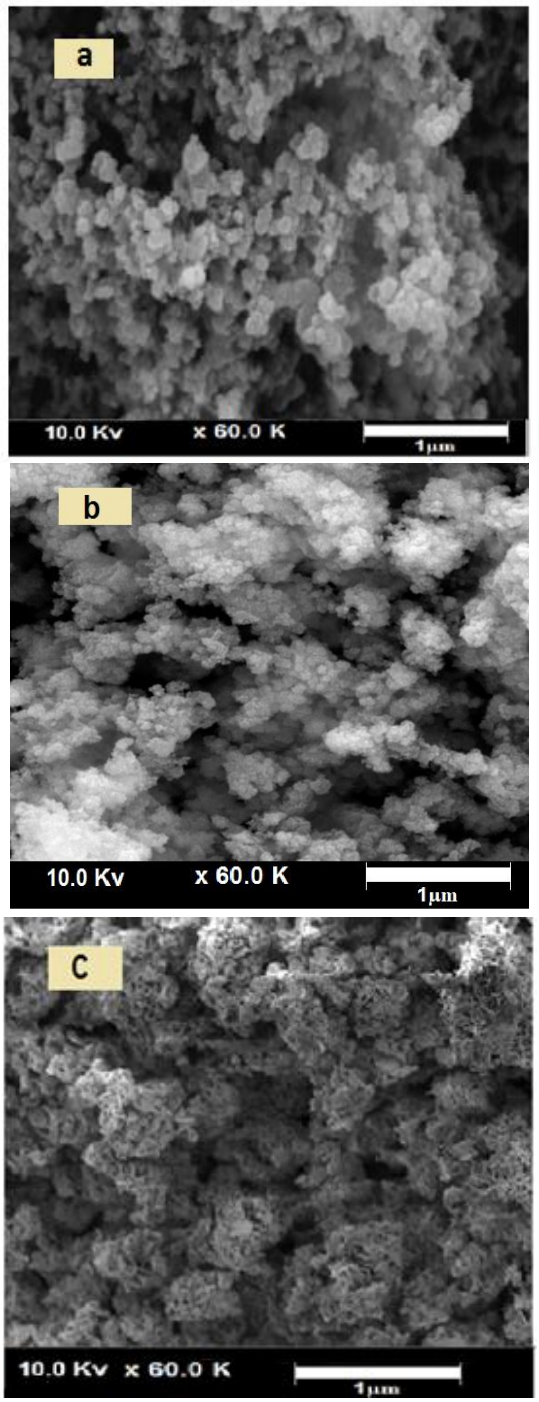

Figure3. *SEM photographs of a) CB, b) MnO_2-CB and c) PANI/MnO_2-CB composites*

Table1. *The element components of CB and MnO_2-CB.*

	C (%)	O (%)	Mn (%)
CB	90.90	9.10	-
MnO_2-CB	28.99	36.97	34.04

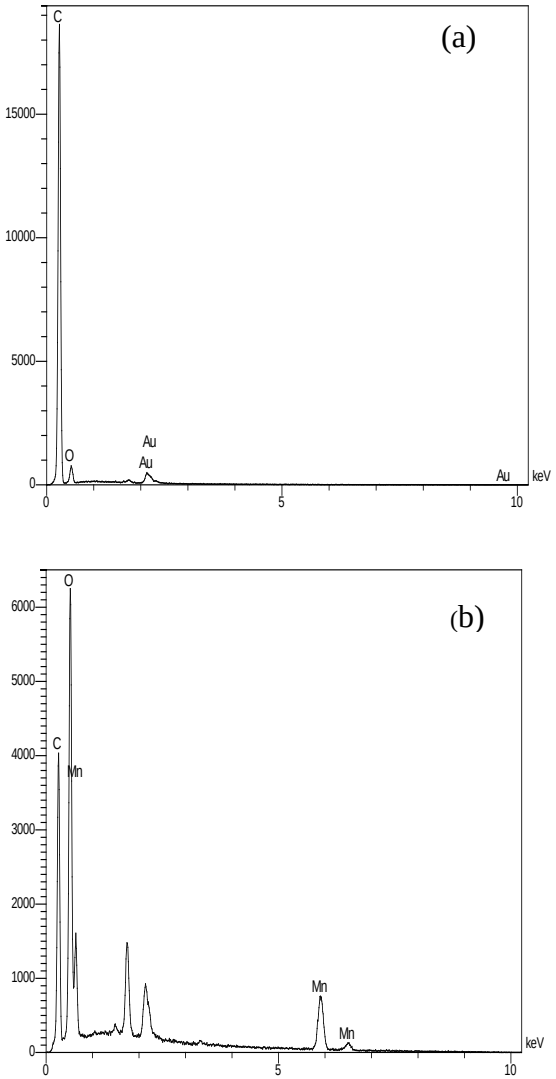

Figure4. *EDS analysis of a) CB and b) MnO_2-CB.*

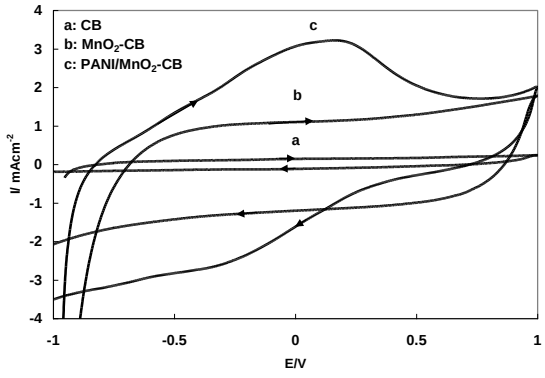

Figure5. *Cyclic voltammetry of a) CB, b) MnO_2-CB, and c) PANI/MnO_2-CB at 10 mV. s^{-1} in 0.5 M Na_2SO_4*

This mechanism mainly describes a surface process, which involves the adsorption/ desorption of alkali cation. It is likely to be

predominant in MnO_2 amorphous (Wang *etal*., 2011, p. 5413).A pair of redox peaks was observed corresponding to the redox reactions of the PANI and exchange between emeraldine and lucoemeraldine states of it. The specific capacitance (C_{sp}, F. g^{-1}) from the CV curves is calculated according to the following equation (Lv *etal*., 2012, p. 1090).

$$C_{sp} = \frac{1}{m.\upsilon.\Delta V}\int I_v \,.\, dv \qquad (2)$$

Where, m is the mass of the grafted CB, *v* shows the potential scan rate, V shows the sweep potential window and I(V) is the voltammetric current on CV curves. For extraction of the specific capacitance from equation 2, the CV was carried out for all nanocomposites at different scan rates. For example, Figure 6 demonstrates the CV curves of MnO_2-CB nanocomposite at different scan rates in 0.5 M Na_2SO_4.

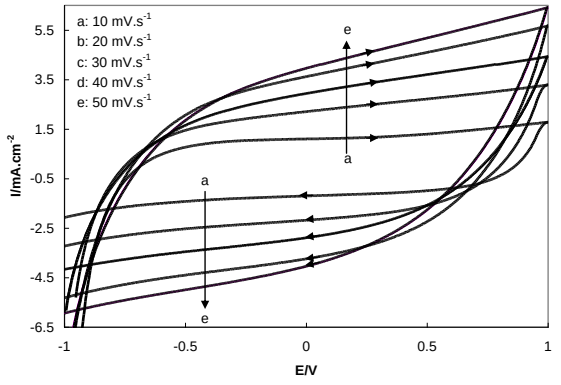

Figure6. *Cyclic voltammetry MnO_2-CB at 10 -50 mV. s^{-1} in 0.5 M Na_2SO_4*

The specific capacitance deduced from the CV curves for the PANI/MnO_2-CB, MnO_2-CB and CB electrodes are 179.8 F. g^{-1}, 121 F. g^{-1} and 44.87 F. g^{-1}, respectively.

3.3. Galvanostatic charge-discharge characteristics

Figure7. shows the charge–discharge curves of PANI/MnO_2-CB, MnO_2-CB and CB nanocomposites measured at a constant current of 0.2 A.g^{-1} within the potential window of 0.0 to 1.0 V vs. Ag/AgCl reference electrode.

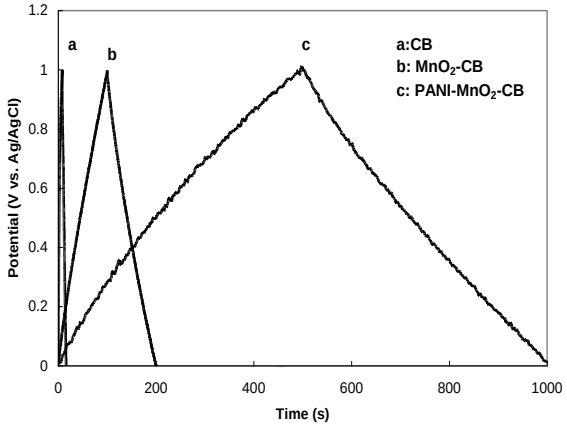

Figure7. *Charge–discharge behaviors of CB, MnO_2- CB, and PANI/MnO_2-CBat 0.2 A/g in 0.5 M Na_2SO_4 Solution*

As shown in Figure7 (a), CB is not in a triangular shape. It is clear that there is a small ohmic drop at the beginning of the discharge, and this states that CB has an equivalent series resistance (ESR) (Hussain & Kumar, 2006, p. 1486).For MnO_2-CB nanocomposite in Figure 7(b) the curves are linear, triangular shaped, very sharp and symmetric. These indicate high coulombic efficiency and reversible behavior. MnO_2-CB and PANI/MnO_2-CB nanocomposites exhibit lower ohmic drop compared with the CB. Their charge/discharge duration increased with the incorporation of MnO_2 and PANI. The specific capacitance of these nanocomposite based electrodes can be calculated according to the following equation (3):

$$C_{sp} = \frac{i}{(dV/dt.m)} \qquad (3)$$

Where, m is the mass of the grafted CB, i is the applied current, dV/dt is the slope of the discharge curve after the IR drop (Wang *etal*., 2011, p. 5413). The specific capacitance of PANI/MnO_2-CB, MnO_2-CB and CB was calculated to be 159.6, 101.2and 36 (F. g^{-1}), respectively.

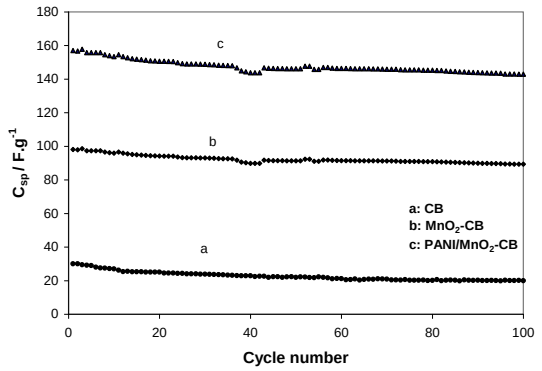

Figure8. *Specific capacitances of a) CB, b) MnO_2-CB and c) PANI/MnO_2-CB as a function of cycle number measured at 0.2 A.g^{-1} in 0.5 M Na_2SO_4 solution*

Cycle stability of PANI-MnO_2-CB nanocomposite was also investigated by galvanostatic charge–discharge tests in 100 cycles and the corresponding results with a current density of 0.2 A.g^{-1}are shown in Figure 8. It can be seen that there is 9% decay in the initial capacitance over 100 cycles. This implies an excellent long-term cycling capability. It is well known that a combination of MnO_2 and other materials, such as conducting polymers, reduce both the MnO_2 dissolution and the mechanical failure and hence lead to excellent electrochemical performance after the number of cycling tests (Wang *etal*., 2011, p. 5413).

The columbic efficiency η of the capacitor can be calculated from the galvanostaticcharge–discharge experiments as follows (Mirmohseni*etal*., 2012, p. 182), (Lv *etal*., 2012, p. 1090).

$$\eta = Q_d/Q_c \times 10 = \Delta t_d/\Delta t_c \times 100 \qquad (4)$$

Δt_c and Δt_d are the charging and discharging times (s), respectively. According to Eq. 4, the average columbic efficiency of PANI/MnO_2-CB is about 96.6%.

3.3.1 Electrochemical impedance spectroscopy analysis

Typical NY Quist diagrams for the electrodes at different DC applied potentials in 0.5M Na_2SO_4 are given in Figure9.

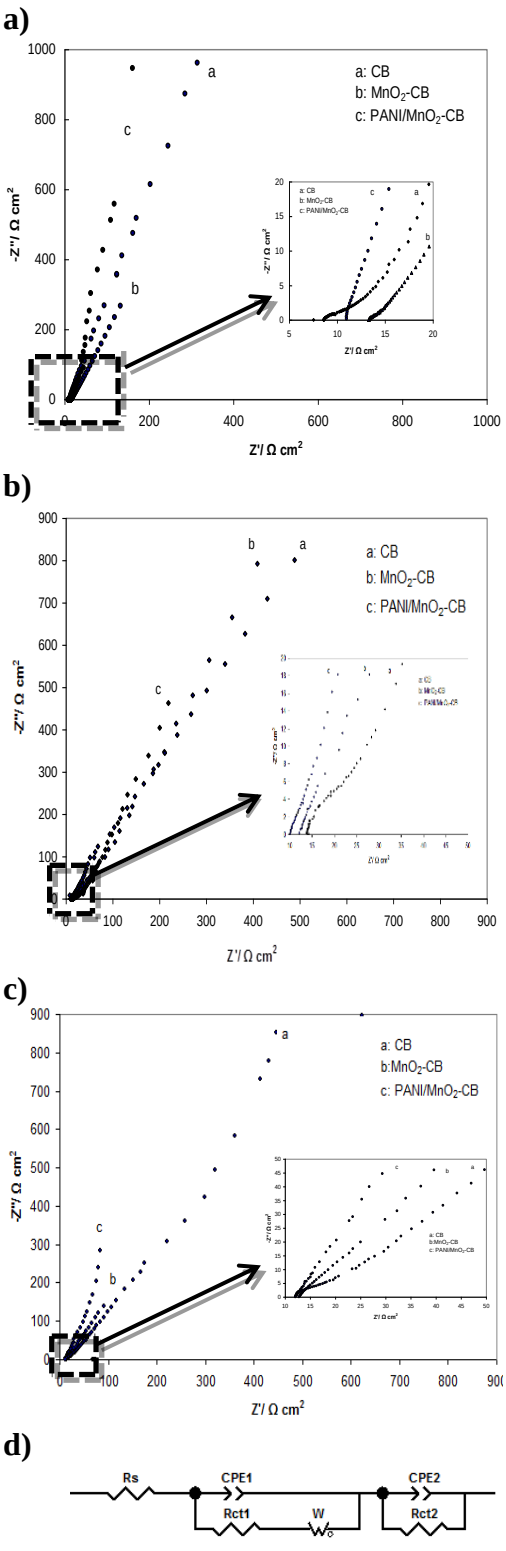

Figure9. *NY Quist plots of the PANI/MnO_2-CB, MnO_2-CB and CB electrodes at different voltages (a) OCP, b) 0.2V and c) 0.4V versus Ag/AgCl) and d) equivalent circuit for the fitting of the EIS spectra of the electrodes*

***Table2**. The best fitting values of the equivalent circuit elements in Figure8 (d) for the impedance data shown in Figure8 (a)-8(c).*

	CB			**MnO_2- CB**			**PANI/MnO_2-CB**		
Element	0V	0.2 V	0.4 V	0V	0.2V	0.4 V	0V	0.2V	0.4V
$R_s(\Omega)$	11.1	12.7	14.1	10.0	12.8	13.2	8.5	12.1	13.9
$Q_1(S.s^{\alpha 1})$	0.07	0.04	0.04	0.12	0.10	0.08	0.11	0.12	0.05
α_1	0.80	0.70	0.69	0.84	0.85	0.83	0.84	0.70	0.68
$R_{ct1}(\Omega.cm^2)$	103	106	110	100	108	110	102	110	105
$W(\Omega.s^{-0.5})$	0.0002	0.0002	0.0003	0.002	0.013	0.030	0.0003	0.2	0.2
$Q_2(S.s^{\alpha 2})$	0.85	0.61	0.50	1.3	0.83	0.60	1.8	0.8	0.5
α_2	0.91	0.90	0.90	0.92	0.90	0.89	0.93	0.92	0.91
$R_{ct2}(k\Omega.cm^2)$	5.60	6.00	5.80	6.50	6.40	6.60	5.10	5.80	5.90
$C_1(mF.cm^{-2})$	114.7	74.29	77.83	192.6	152.2	124.9	174.3	162.6	109.1
$C_2(mF.cm^{-2})$	196.4	151.8	121.2	285.4	215.3	167	357.7	166.7	110.2

In the high frequency range, the intercept at real part (Z′) is a combinational resistance of the ionic resistance of the electrolyte, intrinsic resistance of the substrate, and contact resistance between the active material and the current collector (Wang *etal*., 2011, p. 5413), (Huang *etal*. 2006, p. 1486). The semicircle at high frequency reflects the sum of the electrolyte resistance (R_s) and the charge transfer resistance (R_{ct}) at the electrode/electrolyte interface. These results indicate that the high frequency semicircle can be attributed to the CB charging and discharging process inside the material. At low-frequency, the plots become an almost vertical line, reflecting a capacitive behavior with a low diffusion resistance. In the mid-frequency range, the electrodes behave as a parallel combination of a resistor and a capacitor. The imaginary part of the impedance increases more sharply with decreasing frequency, which is indicative of a faradaic process produced by the redox transitions of PANI and MnO_2 (Gobal & Faraji. 2013, p. 133). The equivalent circuit shown in Figure 9(d) was found to give excellent fits for different impedance spectra of electrodes. The parameters of the equivalent circuit are reported in Table 1. The mean error of modulus is less than 1%, showing that the parameter values obtained from the EIS fitting to the proposed circuit are highly reliable. This equivalent circuit is based on the following equations:

$$Z(\omega) = R_s + Z_1(\omega) + Z_F(\omega) \quad (5)$$

$$\frac{1}{Z_1(\omega)} = \frac{1}{R_{ct1} + Z_\omega} + j\omega C_{dl} \quad (6)$$

$$\frac{1}{Z_F(\omega)} = \frac{1}{R_{ct2}} + j\omega C_F \quad (7)$$

$$Z_1 = \frac{R_{ct1} + W}{1 + R_{ct1} + j\omega C_{dl}} \quad (8)$$

$$Z_F = \frac{R_{ct2}}{1 + R_{ct2} j\omega C_F} \quad (9)$$

$$Z_\omega = R_s + \frac{R_{ct2}}{1 + R_{ct2} j\omega C_F} + \frac{R_{ct1} + W}{1 + R_{ct1} + j\omega C_{dl}} \quad (10)$$

In these equations, ω, R_s, Z_1, Z_F, W, R_{ct}, C_{dl} and C_F are the angular frequency, solution resistance, impedance of electrode/electrolyte interface, bulk faradic impedance, warburg diffusion impedance, ionic charge transfer resistance at the electrode/electrolyte interface, double layer capacitance and bulk faradic pseudo capacitance, respectively. CPE is a nonideal capacitor which its impedance is calculated as follows (Gobal & Faraji. 2013, p. 133):

$$Z_{CPE} = \frac{1}{Y_0 (j\omega)^\alpha} \quad (11)$$

Where Y_0 and α are the parameters that are independent of frequency. The exponent, α,

shows the roughness of the electrode with values from 0 to 1. An ideal CPE shows α= 1 while α= 0 shows resistance and for the warburg behavior α= 0.5. The true capacitance from a depressed semicircle model (i.e. a constant phase element in parallel with a resistor) can be calculated by the following equation (Hsu & Mansfeld. 2001, p. 747):

$$C = \frac{(Q \times R)^{1/\alpha}}{R} \qquad (12)$$

Where C, Q, R and α indicate the specific capacitance (F. cm^{-2}), a constant with dimension (S. s^{α}), ionic charge-transfer resistance (Ω. cm^2) and a constant without dimension, respectively. From Table 2 the values of α are near 1 which indicate the capacitive behavior of the electrodes.

It is obvious from Table 2, that C_2 is greater than C_1 which is in good agreement with the low thickness of the double layer. From Table 2, with increasing the applied potential for all the electrodes, R_{ct2} is greater than R_{ct1}, which is important for redox based supercapacitors. These differences in the values of R_{ct}, result from the redox reactions of PANI or MnO_2 film, which their charge storage mechanism are much faster than of CB. With increasing voltage, the electrode surface becomes more positively charged and movement of anions to the electrode/electrolyte interface is encountered with mass transfer limitations. The sequence of electrodes with respect to the increasing of specific capacitance is PANI/MnO_2-CB > MnO_2-CB > CB.

4. CONCLUSION

PANI/MnO_2-CB and MnO_2-CB nanocomposites were made by the *in situ* direct coating method to deposit MnO_2 on CB; and then PANI coating was coated upon it. Presence of PANI and MnO_2 modified the supercapacitive behavior of CB. The sequence of electrodes with respect to the increasing of specific capacitance is PANI/MnO_2-CB >MnO_2-CB > CB. Increasing of specific capacitance is due to the synergistic effect of PANI and MnO_2.

ACKNOWLEDGMENT

The authors would like to acknowledge the financial support of Iranian National Committee of Nanotechnology in Ministry of Science, Research and Technology and the office of Vice Chancellor in Charge of Research of University of Tabriz.

REFERENCES

1. Simon. P and Gogotsi. Y,"Materials for electrochemical capacitors, "Nature Materials, Vol. 7, (2008), pp. 845-854.
2. Conway. B. E.: "Transition from "Super capacitor" to "Battery" Behavior in Electrochemical Energy Storage, "Journal of electrochemical society, Vol. 138, (1991), pp. 1539-1548.
3. Chen. Y, Wang. J. W, Shi. X. C, Chen. B. Z: "Electrochemical fabrication of porous manganese–cobalt oxide films for electrochemical capacitors"Journal of Applied Electrochemistry, Vol. 45, (2015), pp. 495-501.
4. Liu. F.J., Hsu. T.F. and Yang. H.: "Construction of composite electrodes comprising manganese dioxide nanoparticles distributed in polyaniline–poly (4-styrene sulfonic acid-co-maleic acid) for electrochemical super capacitor, " Journal of Power Sources, Vol. 191, (2009), pp. 678-683.
5. Ghennaatian. H. R., Mousavi, M. F., et al: "Electrochemical investigations of self-doped poly aniline nanofibers as a new electroactive material for high performance redox super capacit*or* "Sythetic, Metals, Vol. 159, (2009), pp. 1717-1722.
6. Mei. L, Yang. T, et al. "Hierarchical mushroom-like $CoNi_2S_4$ arrays as a novel electrode material for super capacitors" Nano Energy, Vol. 3, (2014), pp.36–45.
7. Jian. A, Tripathi. S. K, "Almond shell-based activated nanoporous carbon

electrode for EDLCs" Ionics, Vol. 21, (2015), pp. 1391-1398.
8. Zhang. X, Ji. L, et al: "Synthesis of a novel polyaniline-intercalated layered manganese oxide nanocomposite as electrode material for electrochemical capacitor"Journal of Power Sources, Vol. 173, (2007), pp. 1017– 1023.
9. Konyushenko. E. N and Kazantseva. N. E, et al: "Ferromagnetic behavior of polyaniline-coated multi-wall carbon nanotubes containing nickel nanoparticles" Journal of Magnetism and Magnetic Materials, Vol. 320, (2008), pp. 231-240.
10. Rudge. A, Raistrick. I, et al, "A study of the electrochemical properties of conducting polymers for application in electrochemical capacitors "Electro chimica Acta, Vol. 39, (1994), pp. 273-287.
11. Nam. K. W, Lee. C. W, et al: "Electrodeposited manganese oxides on three-dimensional carbon nanotube substrate: Super capacitive behavior in aqueous and organic electrolytes" Journal of Power Sources, Vol. 188, (2009), pp. 323–331.
12. JM. J. M and Kim. K. M:" Electro chemical properties of MnO_2/activated carbon nanotube composite as an electrode material for super capacitor" Materials chemistry and physics, Vol. 114, (2009), pp. 837-841.
13. Sen. P and De. A:" electrochemical performances of poly (3, 4-ethylene dioxythiophene) - $NiFe_2O_4$ Nano composite as electrode for super capacitor"Electro chimica Acta, Vol. 55, (2010), pp. 4677–4684.
14. Fischer. A. E, Saunders. M. P, et al: "Electroless Deposition of Nano scale MnO_2 on Ultra porous Carbon Nano architectures: Correlation of Evolving Pore- Solid Structure and Electro chemical Performance "Journal of Electro chemical Society, Vol. 155, (2008), pp. A246-A252.
15. Wei. J and Zhitomirsky. I: "Electro synthesis of manganese oxide films "Surface Engineering, Vol. 24, (2008), pp. 40-46.
16. Cheong. M and Zhitomirsky. I: "electrophoretic deposition of manganese oxide films" Surface Engineering, Vol. 25, (2009), pp. 346-352.
17. Cho. S. I and Lee. S. B: "Conducting Polymer Nanotubes: Electro chemical Synthesis and Applications"Dekker Encyclopedia of Nanoscience and Nanotechnology, Vol. 1, (2005), pp. 1-9.
18. Hu. Z. A, Xie. Y.L, et al: "Poly aniline/SnO_2 nanocomposite for super capacitor applications" Materials Chemistry and Physics, Vol. 114, (2009), pp. 990-995.
19. Kim. J. H, Sharma. A. K and Lee. Y. S: "Synthesis of polypyrrole and carbon nano-fiber composite for the electrode of electrochemical capacitors" Materials Letters, Vol. 60, (2006), pp. 1697-1701.
20. Barpanda. P, Li. Y, et al: "Fabrication, Physical and Electro chemical Investigation of Microporous Carbon Poly iodide Nano composites" Journal of Electrochemical Society, Vol. 156, (2009), pp. A873-A885.
21. Fan. L. Z, Hu. Y. S: "High lectroactivity of polyaniline in super capacitors by using a hierarchically porous carbon monolith as a support" Advanced Functional Materials, Vol. 17, (2007), pp. 3083-3087.
22. Yuan. C, Su. L, et al: "Enhanced electrochemical stability and charge storage of MnO_2/carbon nanotubes composite modified by polyaniline coating layer in acidic electrolytes"Electro chimica Acta, Vol. 53, (2008), pp.7039-7047.
23. Kim. K. S and Park. S. J: "Synthesis and high electrochemical performance of polyaniline/MnO_2-coated multi-walled carbon nanotube-based hybrid electrodes"Journal of Solid State Electrochemistry, Vol. 16: (2012), pp. 2751-2758.

24. Wu. K. H, Ting. T. H, Wang. G. P, et al: "Effect of carbon black content on electrical and microwave absorbing properties of polyaniline/carbon black nano composites"Polymer Degradation and Stability, Vol. 93, (2008), pp. 483-488.
25. Shao. W, Jamal. R, Xu. F, et al: "The Effect of a Small Amount of Water on the Structure and Electro chemical Properties of Solid-State Synthesized Polyaniline" Materials, Vol. 5, (2012), pp. 1811-1825.
26. Mirmohseni. A, Seyed Dorraji. M. S and Hosseini. M. G: "Influence of metal oxide nanoparticles on pseudo capacitive behavior of wet-spun poly aniline-multiwall carbon nanotube fibers"Electro chimiaca Acta, Vol. 70, (2012), pp. 182-192.
27. Wang. Y. T, Lu. A. H, Zhang. H. L et al: "Synthesis of Nanostructured Mesoporous Manganese Oxides with Three-Dimensional Frameworks and Their Application in Super capacitors" Journal of Physical Chemistry C, Vol. 115, (2011), pp. 5413-542.
28. Lv. P, Zhang. P, Li. F et al: "Vertically aligned carbon nanotubes grown on carbon fabric with high rate capability for super-capacitors. Synthetic Metals" Synthetic Metals, Vol. 162, (2012), pp.1090-1096.
29. Hussain. A. M. P. and Kumar. A: (2006) "Enhanced electrochemical stability of all-polymer redox super capacitors with modified polypyrrole electrodes"Journal of Power Sources, Vol. 161, pp. 1486-1492.
30. Li. Y, Huang. K, Zeng. D. *et al*: "$RuO2/Co_3O_4$ thin films prepared by spray pyrolysis technique for super capacitors"Journal of Solid State Electrochemistry, Vol. 14, (2010), pp. 1205-1211.
31. Gobal. F and Faraji. M: "Fabrication of nanoporous nickel oxide by de-zincification of Zn–Ni/ (TiO_2-nanotubes) for use in electro chemical super capacitors "Electro chimica Acta, Vol. 100, (2013), pp.133-139.
32. Hsu. C. S and Mansfield. F: (2001) " Concerning the Conversion of the Constant Phase Element Parameter Y_0 into a Capacitance"Corrosion, Vol. 57, (2001), pp. 747-748.